AD-A149 062 GEL DRAWN FIBERS OF POLY(VINYL ALCOHOL)(U) CORNELL UNIV 1/1
ITHACA NY DEPT OF MATERIALS SCIENCE AND ENGINEERING
P CEBE ET AL. 03 JAN 85 TR-2 N00014-83-K-0471
UNCLASSIFIED F/G 11/9 NL

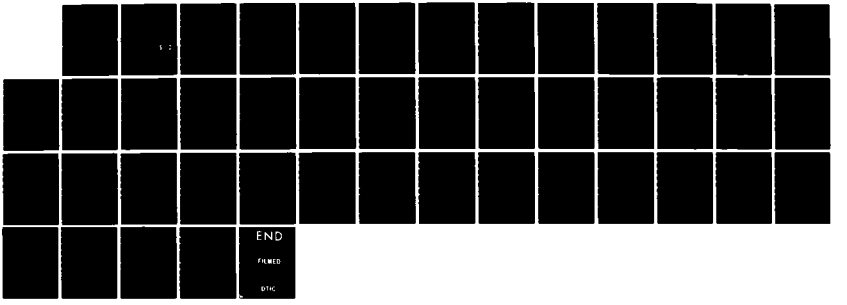

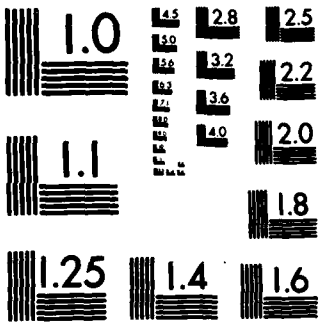

MICROCOPY RESOLUTION TEST CHART
NATIONAL BUREAU OF STANDARDS-1963-A

SECURITY CLASSIFICATION OF THIS PAGE (When Data Entered)

(12)

REPORT DOCUMENTATION PAGE	READ INSTRUCTIONS BEFORE COMPLETING FORM
1. REPORT NUMBER: 2	2. GOVT ACCESSION NO.: AD-A149062
3. RECIPIENT'S CATALOG NUMBER:	
4. TITLE (and Subtitle): Gel Drawn Fibers of Poly(vinyl alcohol)	5. TYPE OF REPORT & PERIOD COVERED: Technical
	6. PERFORMING ORG. REPORT NUMBER:
7. AUTHOR(s): Peggy Cebe and D. T. Grubb	8. CONTRACT OR GRANT NUMBER(s): N00014-83-K-0471
9. PERFORMING ORGANIZATION NAME AND ADDRESS: CORNELL UNIVERSITY, Office of Sponsored Programs, Ithaca, New York 14853	10. PROGRAM ELEMENT, PROJECT, TASK AREA & WORK UNIT NUMBERS: NR 631-843
11. CONTROLLING OFFICE NAME AND ADDRESS: Department of the Navy, Office of Naval Research, Arlington, VA 22217	12. REPORT DATE: January 3, 1985
	13. NUMBER OF PAGES: 40
14. MONITORING AGENCY NAME & ADDRESS (if different from Controlling Office)	15. SECURITY CLASS. (of this report): Unclassified
	15a. DECLASSIFICATION/DOWNGRADING SCHEDULE

16. DISTRIBUTION STATEMENT (of this Report)

This document has been approved for public release and sale; its distribution is unlimited.

17. DISTRIBUTION STATEMENT (of the abstract entered in Block 20, if different from Report)

18. SUPPLEMENTARY NOTES

Submitted for Publication in J. Materials Science

19. KEY WORDS (Continue on reverse side if necessary and identify by block number)

poly(vinyl alcohol), fibers, fiber drawing, gelation, modulus, crystallinity, crystal orientation.

20. ABSTRACT (Continue on reverse side if necessary and identify by block number)

Semi-crystalline gels of several samples of poly(vinyl alcohol) were made from solutions in which the polymer concentration varied from 2.0 to 15.0%. Entanglement density in the material was in this way reduced from the melt entanglement density. When gels were partially dried and drawn isothermally the maximum draw ratio increased with drawing temperature up to 11-14 at 140-180°C. A melt cast film could be drawn to 6.8 times at 140°C. Drawn material had a crystallinity of 55-80%, while that of isotropic material was 20-55%

DD FORM 1 JAN 73 1473 EDITION OF 1 NOV 65 IS OBSOLETE
S/N 0102-LF-014-6601

SECURITY CLASSIFICATION OF THIS PAGE (When Data Entered)

20 Abstract (continued)

Gels of lower initial concentration (lower entanglement density) could be drawn to greater extensions at a given draw temperature and had better mechanical properties. Young's modulus increased with draw ratio to values very close to those for polyethylene fibers drawn by the same amount. Young's modulus was independent of drawing temperature or degree of crystallinity but on comparing drawn gels of the same draw ratio, crystallinity and crystalline orientation, those of lower entanglement density had higher Youngs modulus.

OFFICE OF NAVAL RESEARCH

Contract N00014-83-K-0471

Task No. NR 631-843

TECHNICAL REPORT NO. 2

Gel Drawn Fibers of Poly(vinyl alcohol)

by

Peggy Cebe and David Grubb

Prepared for publication

in the

Journal of Materials Science

Cornell University

Department of Materials Science and Engineering

Ithaca, NY. 14853

January 3, 1985

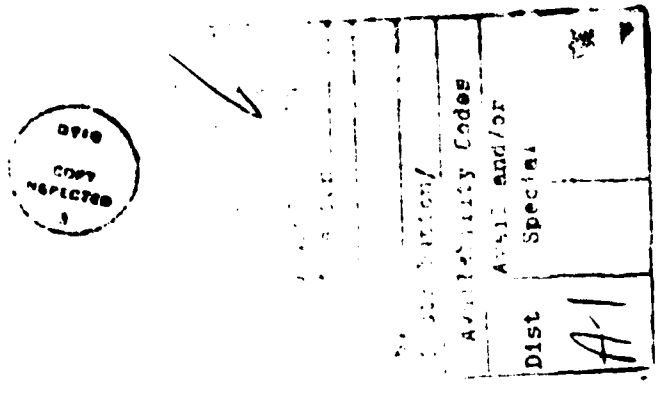

GEL DRAWN FIBERS OF POLY(VINYL ALCOHOL)

Peggy Cebe* and David Grubb

Dept of Materials Science and Engineering

Cornell University

Ithaca N.Y. 14853

ABSTRACT

Semi-crystalline gels of several samples of poly(vinyl alcohol) were made from solutions in which the polymer concentration varied from 2.0 to 15.0%. Entanglement density in the material was in this way reduced from the melt entanglement density. When gels were partially dried and drawn isothermally the maximum draw ratio increased with drawing temperature up to 11-14 at 140-180°C. A melt cast film could be drawn to 6.8 times at 140°C. Drawn material had a crystallinity of 55-80%, while that of isotropic material was 20-55%. Gels of lower initial concentration (lower entanglement density) could be drawn to greater extensions at a given draw temperature and had better mechanical properties. Young's modulus increased with draw ratio to values very close to those for polyethylene fibers drawn by the same amount. Young's modulus was independent of drawing temperature or degree of crystallinity but on comparing drawn gels of the same draw ratio, crystallinity and crystalline orientation, those of lower entanglement density had higher Youngs modulus.

* Now at Jet Propulsion Laboratory, Pasadena, CA 91109.

1. INTRODUCTION

Published work on the production of high modulus fibers from flexible linear polymers has been largely concerned with polyethylene (PE) and one reason for this is the high Young's modulus along the chain axis, of 250-300 GPa.[1,2] (For a recent review of all such work, see Ohta.[3]) Ultra-high values of fiber tensile modulus in PE (over 50 GPa) were first achieved by hot drawing melt crystallized material.[4-6] It was found that modulus was a monotonically increasing function of draw ratio (λ) and that other processing variables had much smaller effects than λ.[5,6] Thus if a method could be found to draw any given starting material to high λ, the result should be a high modulus fiber (unless the temperature is too high and the molecules can relax so that the process is only the extensional flow of a liquid).

Pennings and others have formed high modulus PE fibers from dilute solutions of high molecular weight polymer at the surface of a rapidly spinning rotor.[7-9] Smith and co-workers have obtained high modulus fibers (E = 90-100 GPa) by drawing PE gels.[10-13] Gels were made from solutions of a range of initial concentrations, C. High modulus fibers having high draw ratios λ were obtained from high molecular weight material when the initial solution concentration was low, even if the gels were completely dried before drawing. The maximum value of λ obtainable under given conditions, λ_{max} was found to be proportional to $C^{-1/2}$, just as predicted from the extensibility of the entanglement network.[13] Smith and Lemstra concluded that the entanglement density in solution, reduced to $\xi_e' = C.\xi_e$ from its melt value ξ_e is preserved in the gel and controls drawing behavior. The moduli of drawn gels show trends similar to those of other drawn PE fibers. In particular, the modulus depends primarily on λ and all other variables such as draw temperature, molecular weight and sample history (initial solution concentration or thermal treatment) are much less important.[14]

Further work on fibers grown from dilute solutions and drawn from gels has established a connection between the formation of high modulus fibers at high temperature by the surface growth technique and the presence of surface adsorbed layers which can form gels.[15] Such fibers, although prepared from a mobile dilute solution, can thus be described as stretched gels. It has also been shown that shish-kebab crystals, typically seen to form in stirred dilute solutions, are an intermediate state in gel drawing.[16] Single crystals formed from quiescent dilute solution should have very low entanglement density and mats of single crystals have been drawn to $\lambda > 300$, forming high modulus fibers.[17] When a single crystal mat is melted, the melt viscosity is very low, and it increases to a normal value over a period of time.[18] This is direct evidence for the reduction in ξ_e by solution processing, and the gradual re-establishment of the equilibrium value in the melt.

Conditions for successful drawing of melt crystallized material to high λ are the same as those for disentanglement during drawing, that is, slow drawing at high temperature of material of moderate molecular weight.[4-6] Achievement of high draw ratio can then by itself be taken as evidence for reduced entanglement density ξ_e' [19] and ξ_e' is the common feature in high modulus fibers from PE, controlling λ and thus modulus.

To get high modulus fibers from other polymers we should look for high draw ratios and reduced entanglement densities, and gelation is the best controlled way to reduce entanglement density. Peguy and Manley [20] have used this route for polypropylene, drawing dried gels [21] originally formed at 1% polymer concentration to $\lambda = 57$. The resultant fibers have nearly the theoretical modulus and strength of polypropylene, but the helical conformation of the molecules in the crystal make this theoretical modulus much less than that of PE at only 41 GPa.[22] The 'other polymer'

considered here is poly(vinyl alcohol), (PVA) chemically a near relative of PE. PVA has an all-trans chain conformation in the crystal and a crystal structure very similar to that of PE so the theoretical Young's modulus in the chain direction is very high. It also has high crystal relaxation and melting temperatures compared to PE so that a higher use temperature and better creep resistance may be expected. For comparison the crystalline relaxation occurs at 140°C in PVA and 70°C in PE, while crystals melt at 240°C in PVA and 140°C in PE. The transition temperatures in PVA are so much higher because of the strong polar interaction between the chains.

Strong interaction between chains is expected to make the drawing behavior very different to that of PE and the polar hydroxyl groups also cause the material to be sensitive to water. Much of the material sold as PVA is water soluble, but this is actually a copolymer of vinyl alcohol and vinyl acetate. PVA is produced by the hydrolysis of poly(vinyl acetate) and a copolymer of low crystallinity is the result unless the reaction goes to completion. The crystalline homopolymer PVA does not dissolve in water except at high temperature, but just as for polyamides, the mechanical properties are strongly affected by water absorption. Several groups have investigated the gelation of PVA from various solvents [23-27] and Yamaura and co-workers have studied crystallization from stirred solution and gelation as a function of the chemical structure of the PVA (molecular weight, residual ester group content and distribution, branching, tacticity and head-to-head content).[28-31] Here we present the first results in a study of gel drawing of PVA at temperatures near the crystal relaxation temperature.

2. EXPERIMENTAL

2.1 Fiber Production

The starting materials used were of two types: PVA powders nominally 99-100% hydrolyzed and of weight average MW 115,000 and 86,000 (SPS Inc.) and high tenacity PVA fibers kindly supplied by Kuraray Co. and by P.J.Lemstra. Gels formed from these materials were named D,F,K and L during this study. Viscometry of the four samples in a 1:3 mixture of ethylene glycol and water at 35°C showed that the molecular weights of the K and L fiber samples lay between those of the powders and were approximately 93,000 and 87,000 respectively. IR and NMR analysis showed that all the materials were essentially atactic.

PVA powder was dissolved in a 2:1 mixture of ethylene glycol and water at 135°C. After a few hours the hot solution was poured onto a glass tray where it gelled on cooling. The fibers could not be dissolved in this way, so they were dissolved in pure ethylene glycol at 195°C. The temperature of the solution was lowered to just below 100°C and water added to give the required 2:1 ratio. After homogenizing the solution at 135°C it was gelled in a glass tray as before. At room temperature syneresis occurred for several days. The drying process was then continued by heating to 60°C in a vacuum oven. When dry;-gels were transparent, brittle and difficult to handle. Dried gels were cut from the glass and allowed to absorb a little water before being punched into tensile specimens with a gauge length of 0.5 inch. These specimens were drawn without re-drying at elevated temperatures in an Instron tensile tester at 10 inches/minute. Extension was measured from the separation of marks on the gauge section for samples that were not taken to failure. Extension of samples that were drawn to break was obtained from crosshead movement.

2.2 Fiber Characterization

After drawing, the center of the gauge section was cut out and dried in methanol at room temperature to remove the residual solvent which was about 17% by weight of the drawn fiber. The stress-strain curves of the dried drawn gels were obtained at room temperature using a crosshead speed of 0.005 inches/minute. This mechanical test was not performed in a controlled atmosphere so reabsorption of water is likely. Young's modulus was calculated from the slope of the curve in the region below 0.3% strain.

Thermal analysis was performed using a Perkin-Elmer DSC-2C. Crystallinities were calculated from the area of the fusion peak using 37.3 cal/g as the heat of fusion of PVA crystals.[32] Drawn samples were tested at a heating rate of 20°C/min, and were allowed to contract freely during heating. Wide and small angle X-ray diffraction patterns were obtained using flat plate geometry in a Statton camera. Fiber orientation of crystalline PVA in the drawn samples was estimated from the angular spread of the (110) reflection.

Optical microscopy with a Mettler hot stage was used to examine the retraction of the drawn gels upon heating near the melting point. Two testing procedures involving different sample histories were used to distinguish the effects of heating rate on retraction. To get the retraction as a function of temperature at a fast heating rate, many pieces were cut from a single fiber and each was placed in the hot stage when it was equilibrated at the required temperature. In the slow heating test, a single fiber was heated from room temperature to the melting point, and its length was continuously measured. Shrinkage was described as a retraction, R, defined as:[33]

$$R = (L_d - L_s)/(L_d - L_o)$$

Where the sample length is L_o before drawing, L_d after drawing, and L_s after

shrinking.

L_o was not measured but calculated as L_d/λ giving:

$$R = (1 - L_s/L_d)/(1 - 1/\lambda)$$

3. RESULTS and DISCUSSION

3.1 Drawing of PVA Gels

Typical stress-strain curves obtained during hot drawing are shown in Figure 1. Figure 1a contains curves obtained from gels made from PVA powder of MW 115,000 (D-gels) at a range of concentrations and drawn at the same temperature. Figure 1b contains curves obtained from L-gels of initial concentration 4.2% drawn at a range of temperatures. Figure 1a shows that yield stress and neck formation are relatively insensitive to the initial concentration of the gel, but the orientational hardening and thus the stress at high strains increases with concentration. The apparent reversal of this trend at 15% concentration is due to slippage at the grips. Higher concentration gels were thicker and difficult to grip at the high temperatures of drawing. Figure 1b shows that both the yield stress and the rate of strain hardening decrease as the drawing temperature increases. The failure at $\lambda = 7$, $T_d = 168^oC$, seems premature and may be due to surface defects. To get very high draw ratios, the drawing stress should remain fairly constant [11] so that Figure 1b shows that a high drawing temperature will be required.

In Figure 2a the maximum draw ratio λ_{max} is plotted as a function of the drawing temperature for various concentrations of D-gels In this series of tests, all samples were drawn to failure, so λ_{max} was calculated from the crosshead movement. λ_{max} represents an average over the entire drawn portion of the fiber, and this includes

the less highly drawn material adjacent to the grips. When values of λ_{max} were compared to the extension of the highly drawn central region of unbroken samples, λ_{max} was 5-10% smaller. Thus λ_{max} is a lower limit to the extension of the fiber during drawing, and when higher λ values are quoted later, they refer to the highly drawn central portions. λ_{max} goes through a plateau near the glass transition temperature (86°C) then increases as the temperature approaches the crystal relaxation temperature (140°C). The anomalous behavior of the 15% gel, which draws to nearly 4 times at room temperature, is due to solvent retention. This sounds odd, for the low concentration gels contain much more solvent to begin with. However the casting of a low concentration gel results in a thinner film after drying so that by the time a film originally 2% has dried to 15% solids concentration it is much thinner than we can cast a 15% gel. It thus continues to dry at a faster rate. The plasticization of the 15% gel will reduce the glass transition temperature so that the plateau in λ_{max} will also be reduced in temperature. However as the temperature rises solvent will be extracted from the sample during temperature equilibration and drawing, particularly as the heating is by forced hot air. At higher temperatures of drawing the solvent effect is reduced and the trend shown is for the higher draw ratios to be achieved with lower concentration samples. Similar plots of λ_{max} versus drawing temperature for some gels made from fiber starting materials are shown in Figure 2b. In most cases λ_{max} increases continuously with drawing temperature, with a slight plateau in evidence for the K-gels of concentration 2.1%.

When gels were drawn at 180°C, the maximum draw ratio obtained from high concentration gels increased, but only to λ=12. The fibers formed in this way had very low Young's modulus (1-3 GPa) indicating that the molecules were relaxing during drawing, or possibly that chemical degredation of PVA was affecting the properties. Two of the L-gels, 2.4% and 4.2%, had a peak in λ_{max} (at about 140°C) and a

significant decrease, to less than 10, at the highest temperatures. These are not shown in Figure 2.b, but the L-gel of concentration 4.2% is shown to fail at low λ in Figure 1b. Similar behavior was seen by Smith and Lemstra in gels of PE [34] and attributed to the effect of residual solvent. These L-gels had a slightly higher than normal extension at room temperature and a longer region of strain hardening before failure which indicates plasticization, but the 15% gel (Figure 2a) which is clearly plasticized does not show the same effect. The premature failure of these particular L-gel samples at high temperatures may have been due to a high concentration of surface defects.

In Table 1, maximum theoretical and experimental draw ratios are listed for all the gel concentrations used in this study along with values for l_e' and d'. where l_e' and d' are the chain contour length between entanglements and the rms distance between entanglements, respectively. The theoretical draw ratio of a three dimensional network is given by:

$$\lambda_{th} = l_e'/(3^{1/2}d')$$

The factor of $3^{-1/2}$ comes from consideration of the average projection of the network strand on the tensile axis. In a gel formed from a solution of polymer volume fraction C, $l_e' = l_e/C$ and $d' = d/C^{1/2}$ where l_e and d relate to the 'undiluted' network which exists in a melt. In-PVA, l_e = 14 nm and d = 4.65 nm. These numbers are derived from a molecular weight between entanglements of 2400 [32] and a ratio between end-to-end distance and MW of 0.95 A/(amu)$^{1/2}$. For gels drawn at temperatures above 140°C, experimental draw ratios range from 11 to 14. In all cases the draw ratios observed are larger than those predicted by the theory of entanglement limited drawing, but the range observed is very narrow compared to the range of 1.7 to 12. for λ_{th}. The last two rows in Table 1 show the critical overlap concentration c^* for the extreme values of MW used here. At c^* the molecules are only just entangled and

drawing to λ_{th} from c^* would fully stretch out the molecules. At concentrations less than c^* cooling the solutions should lead to suspensions and not gels and no gels could be formed from solutions less than 2%. If there are only weak intermolecular interactions then drawing to extensions greater than the λ_{th} derived from c^* should lead to loss of strands from the network and loss of strength. The limiting draw ratio in Table 1 could be due to this limitation of the material, as disentanglement at high draw ratios could lead to strand loss, weakness and failure even in gels formed well above c^*. In that case, an increase in molecular weight would allow higher draw ratios. Alternatively, there could be a limitation imposed by the drawing system.

As published work on gel drawing relates chiefly to PE it is clear that the behavior of PVA should first be compared to that of PE. The trends shown in Figure 1 are very similar to those of PE, that lower initial gel concentrations and higher draw temperatures give rise to flatter stress-strain [13] curves (less strain hardening) and higher draw ratios with a few exceptions discussed above. However the PE gels could be drawn to much higher λ_{max} [34] and the variation of λ with concentration was much closer to that predicted theoretically. Often in PE gel drawing the λ_{th} used is just l_e'/d' without the $3^{1/2}$ geometric factor. This is because at temperatures just above the crystal relaxation temperature of 70°C both the solid melt crystallized material and gels of all concentrations could be drawn to l_e'/d'. In PVA l_e'/d' is 15-20 for concentrations of 4-2%, so few of the low concentration gels reached l_e'/d'. In PE drawing at high temperatures can give a much higher λ. For example the melt crystallized material can be drawn to 40 times [4-6] gels have been drawn up to 100 times [35] and single crystal mats up to 350 times.[17] The $3^{1/2}$ factor is not very important since neither formula takes account of strand length distribution or entanglement point slippage or any of modern network theory. It is mentioned because

its use here could lead one to believe that PVA and PE entanglements densities are more different than they are. λ_{th} for PE has been given as 3.7 [13] when calculated on the same basis λ_{th} for PVA is 3.0, not 1.8 as in Table 1.

Several reasons present themselves for the reduced maximum drawability of the PVA gels in this study. 1) Inter-chain bonding in PVA is by relatively strong hydrogen bonding, and this may inhibit mobility during drawing even at temperatures above the crystal relaxation temperature. The chains will then not be able to disentangle during drawing and λ will be limited to λ_{th} or less if the molecular chains cannot move easily through the crystals. 2) All the very highest values of λ in PE have been obtained with high molecular weight material where c^* is low and the draw ratio to extend the molecular chains fully is not much exceeded. Thus the starting materials used here may simply be of too low molecular weight for ultra-high draw ratios. 3) The drawing oven required some equilibration after a sample was inserted so that each sample had 6-8 minutes at high temperature before drawing. This may have allowed some re-entanglement which would tend to reduce differences between initial concentrations and to reduce λ. It did allow relaxation of the gel within the grips and slippage at high temperature was common.

We know that 1) is not an absolute limitation of the material because samples of high initial entanglement concentration can be drawn to high λ producing fibers of good mechanical properties by the process of zone drawing, where the sample sees a very high temperature for a very short time.[3,36-38] Reason 2) is not wholly convincing because PE of MW 100,000 can be drawn to 35 times [3,4] which is about 30% over l_e'/d' or 60% over λ_{th}. If PVA of the same MW could be drawn to the same amount, we would have λ_{max} of 25. The <u>gel</u> drawing of PE, however, has only been reported with much higher molecular weight material. The practical problems of 3) would be eliminated by

zone drawing.

3.2 Fiber Characterization

Since the purpose of fiber production is to get stiff and strong material, and only the crystalline phase is stiff, it is important to know the crystallinity of the fibers and how this varies with preparation parameters. Total crystallinity was obtained from the area under the melting endotherm in the DSC, so there is no distinction made between different forms of crystal - lamellar or fibrillar or different arrangements of crystals. In PE fibers the Young's modulus varies while the total crystallinity remains roughly constant, and the increase of Young's modulus is explained by a change from mechanically isolated to mechanically connected crystals (which may or may not be physically connected into larger crystals).[4,19,39,40] A change from lamellar to fibrillar crystals [7,8] will have a similar mechanical effect. Nevertheless, measurement of total crystallinity is an important first step in modelling modulus.

After drawing gels of PVA the melting endotherms became much narrower and melting points increased by an average of 6.5°C indicating that more perfect crystals are formed during drawing. Total crystallinity versus λ is plotted in Figure 3a for three sets of samples. Isotropic undrawn dried gels have crystallinities ranging from 40 to 55%. The range in drawn samples made from the same starting material is 53-79%. After the drawn fibers had been melted in the DSC they were quenched to room temperature and retested. The crystallinity of this melt quenched material is much less than that of the original gels, and also much less than that of the materials in their as-received state, powder or fiber.(Figure 3a) It is not surprising that rapid cooling in the presence of solvent to form the gel allows more molecular motion than rapid cooling from the melt in the absence of solvent so that greater crystallinity

can develop. This greater mobility will not persist at low temperature when crystals have formed so that the solution entanglement density can still be permanently 'frozen in' in the gel at room temperature.

In Figure 3a the crystallinity of the drawn fiber shows almost no variation with λ. A slight tendency for crystallinity to increase with λ is supported mainly by the two samples with the largest values of crystallinity and λ. There is no pattern of variation for the crystallinity of samples formed by quenching gels nor does the crystallinity of the original unoriented gel seem to have any effect. This indicates that chemical differences in the starting materials and chemical degradation during drawing are not important, at least for crystallinity.

The effect of drawing temperature, T_d, on crystallinity is shown in Figure 3b. Annealing experiments were performed in the same temperature and time regime as hot drawing to determine if crystallinity changes could be attributed to thermal effects alone. Undrawn gel samples were heated in the DSC to the annealing temperature and held for 10 minutes, then cooled and tested. Results for crystallinity and melting point of annealed gels are shown in Table 2. Melting points of the annealed gels are very close to those of the unannealed gels. Crystallinities showed a definite increase as the annealing temperature increased. Lower concentration gels experience the greatest change in crystallinity at 115°C, the lowest annealing temperature. Higher temperatures cause little further change in crystallinity for the low concentration gels. In contrast, the high concentration gels do not change in crystallinity until the temperature is much higher and nearly all the increase occurs at 160°C. This dependence on concentration gives a range of crystallinities obtained by annealing which is shown by the lines in Figure 3b.

All of the drawn samples have crystallinities greater than that obtainable by annealing, Table 3. (The three points which fall between the lines in Figure 3b all have crystallinities greater than that of there annealed counterparts, as can be verified from Table 2). We conclude that hot drawing improves the crystallinity of the material to a greater extent than simple annealing does. Annealing also has less effect on crystal perfection, since the melting point hardly increases on annealing, but increases very significantly on drawing as shown in Table 3. Shrinkage results to be described below show that the increase in melting point is not due to superheating or constraints on the fiber.

Results of Young's modulus versus λ are plotted in Figure 4a,b for a range of gel concentrations, from data in Table 3. When all the data is included, Figure 4a, the plot contains a broad band of points with a clear positive slope. One reason for the large scatter in E is the formation of voids during drawing. Stress-induced whitening was clearly visible when samples were drawn at low temperature, and optical microscopy of samples drawn at 140°C indicated the presence of elongated voids not present before drawing. Interchain bonding in PVA is strong even at high temperatures, as is shown by the lack of disentanglement during drawing and the small reduction in drawing stress when the drawing temperature is increased from 111 to 168°C (Figure 1b).

Restricting the data set to draw temperatures from 140 to 165°C and gel concentrations less than 5% gives Figure 4b, a much more well defined dependence of Young's modulus on λ. Included in Figure 4b are six points for drawn melt crystallized PE taken from the literature.[6] They are there purely for comparison. They show that ultra-high values of the Young's modulus are not to be expected at these limited draw ratios. The observed maximum value of 20 GPa is a respectable

figure for a polymer fiber, it is close to the Young's modulus of commercial PVA tire cord [ref], but it is less than 10% of the theoretical crystal Young's modulus for PVA.

Figure 4b also makes it clear that the data so far obtained are insufficient to prove or disprove the suggestion that the modulus of all entanglement limited drawn fibers will give a straight line if plotted as $1/E$ versus $1/(\lambda^2)$.[19] This plot can only be superior to the direct plot of E against λ if the direct plot gives a curve sigmoidal in shape, levelling off at very high modulus as some saturation value is approached. The curve in Figure 4b is still increasing in slope at the draw ratios accessible, and the same is true for PE data at $\lambda<25$.

Figure 5 is a direct check on the correlation between crystallinity and Young's modulus. Crystallinity lies in the range 53% to 65% while Young's modulus varies widely from 4.7 to 15 GPa. There is essentially no dependence of E on λ for the PVA gels, although the very highest moduli were obtained at the highest crystallinities. As in Figure 3a, two fibers stand out, that made from an L-gel of 2.1% concentration with $\lambda=12.0$ and that from a D-gel of 2.0% with $\lambda=13.6$. WIthout these one would say that there is no relation between crystallinity and λ or between crystallinity and Young's modulus. With these fibers of the highest observed λ, there is some indication that crystallinity may begin to change at higher draw ratios.

Figure 5 can also be used to make general comparisons between the various starting materials. All 4.2% L-gels have moduli below 8.4 GPa, the 2.4% gels have moduli in the range 8.1 to 1.8 GPa and the 2.1% L-gels have the highest moduli, 12.4 to 17.2 GPa. Considering the K-gels in the same way, at 3.8% the modulus range is 4.7 to 10.5 GPa, but the lower concentration 2.1% gels are in a higher range at 10.9 to 13.1 GPa. It would seem clear that Young's modulus increases as initial concentration

decreases. A closer look shows that the reason for this trend is that the lower concentration materials can be drawn to higher λ and higher λ gives higher modulus. If we were to take the same modulus data as presented in Figure 4a and compare different concentrations at the same λ the trend would be the opposite, higher concentration gels having the higher modulus. A theory of the Young's modulus of drawn gel fibers [19] has the entanglements acting as defects in the fiber, reducing the modulus so that lower concentration gels should have higher Young's modulus. However, this theory relates to the fully oriented state, which is not arrived at until the gel is drawn to λ_{th}. If fibers are compared at the same draw ratio, which produces full orientation only for gels of high concentration, the material of low concentration, not fully drawn, may well show a lower modulus.

Crystal orientation in the drawn fibers was measured by WAXD as the angular range of the arc of the strong (110) reflection and the results are shown in Figure 6. Lines in Figure 6a,b connect data points from gels of the same starting material and initial concentration (entanglement density). In Figure 6a the orientation angle is plotted against draw ratio, λ. At low draw ratio there is a large spread in orientation angle which narrows as λ increases. The orientation continues to improve substantially in the range of draw ratio covered here. In PE fibers, ultra-high modulus is not achieved until drawing proceeds at nearly perfect orientation. Figure 6a does not show any significant difference in orientation angle between different starting materials. Figure 6b contains the same orientation data plotted against the Young's modulus of the fiber. Now the different materials and concentrations are well separated. At a given orientation angle fibers of lower concentration have a higher modulus. The four points in Figure 6a at draw ratio near to 12.2, for example, have orientation angles between 12 and 14.5. These four points replotted in Figure 6b are no longer together as the moduli of these samples range

from 8.5 to 15.1 GPa. Thus draw ratio is not the only factor controlling modulus. Solution concentration, i.e. entanglement density, has a direct effect in that when gels of the same draw ratio and crystalline orientation are compared, those with a reduced entanglement density have the higher Young's modulus. This is true only when all the gels are drawn to $\lambda > \lambda_{th}$ (remember that at low λ the high concentration gels have higher modulus) and when the orientation angle has still not reached its limit. Orientation angle is not considered an important variable in PE fibers because it is alwalys very small, although improvements in the perfection of crystal orientation are still seen at extremely high draw ratios.[35]

Another structural method of investigating fibers is small angle X-ray scattering. Uniaxially drawn fibers normally show a two spot pattern indicating the presence of a lamellar structure aligned in columns. As the draw ratio and Young's modulus increases in PE the intensity of this SAXS pattern decreases, although the peak position (long spacing or crystal thickness repeat distance) does not change much. The same type of pattern was obtained from the drawn gel fibers of PVA and the long spacing remains in the range of 11-13 nm for all draw ratios. This is close to the range of long spacing that has been seen for PVA single crystals.[41] Only drawing at extremely high temperature has an effect on the long spacing. A 6.2% D-gel was drawn to $\lambda = 12.2$ at 180°C and its long spacing increased from 11 to 15 nm.

An important feature of fiber drawing is the extension of the entanglement network, so the crystal size and orientation as determined by X-ray diffraction is not as important as the molecular or network extension, M. Shrinkage of the drawn sample back to an isotropic relaxed state is the primary indication of molecular extension.[42-44] M is defined as (drawn length)/(shrunk length), L_d/L_s.[33] The shrinkage data was used to derive M and retraction, R, described in section 2.2, which is

convenient for the comparison of samples of different draw ratios. Retraction and molecular extension are related by:

$$M = 1/(1 - R(1 - 1/\lambda))$$

The calculations of molecular extension depend on the fiber retracting without competing relaxation of the extension. When fibers of the same draw ratio were subjected to different heating programs, the measured retraction varied considerably, as shown in Figure 7. Solid lines in Figure 7 connect data from the fast heating test, where each point comes from a different small sample heated directly to the test temperature. The dashed lines connect data from slow heating tests, where one sample was heated continuously and slowly. Irregularities in retraction at high temperatures such as reduced retraction for temperatures above the melting point, are present only in the fast heating tests. Absolute retractions, however, are much lower in the slow heating tests. This indicates that the slow heating allows some relaxation of the oriented molecules. This hypothesis was tested by heating one sample, D27 in Figure 7, continuously to the melting point, but at a much faster rate than used for the slow heating tests. This did not allow many measurements of length to be made, but at the melting point the retraction is higher than that of the slow test and lower than that of the fast test. As retraction thus depends on heating rate, the fastest rate should be used, and the observed retraction is still only a lower limit, since with even faster rates, greater retractions might be achieved.

All fibers retract over a narrow range of temperature, and the great part of the observed retraction is over when the temperature reaches the melting point as found by thermal analysis. This gives some confidence that the measured melting points were of the freely retracting fibers, not strongly affected by constraints. Gels drawn from fiber starting material do continue to retract above the melting point, so that the

maximum retraction may be seen at 250°. The spread of retraction is consistent with the spread in the melting endotherm seen in these materials.

Table 4 summarizes the retraction measured for a range of drawn samples, and the molecular extension, M, derived from R. The table also includes M/λ, a measure of efficiency of molecular extension. (This was called R'' in ref 33.) The error in M is about M times the error in R so that small errors in measurement of the final length after shrinkage can be serious. There are no clear trends of retraction or drawing efficiency with draw ratio, sample type or drawing temperature above 100°C. All of the samples drawn at high temperature (except possibly the first in Table 4) show drawing efficiencies M/λ of 40 to 70%. It is probable that the particular values found depend upon experimental conditions, primarily the heating rate but also the sample size due to constraint and surface tension effects.

4. CONCLUSIONS

Coherent and homogeneous gels of PVA can be made from ethylene glycol/water solutions at concentrations above the overlap concentration c^*. When partially dried these gels can be drawn in the temperature range 140-165°C with effective molecular extension to draw ratios of up to 14. This is a much larger extension than can be achieved by hot drawing of the melt crystallized material, but a higher draw ratio, 19, has been obtained by zone drawing at 240°C. Structural studies show an improvement in crystallinity and in crystal perfection on drawing. At draw ratios of 10-14 the crystalline orientation is still improving with λ and there is still a strong SAXS peak indicating the presence of lamellar structures. The Young's modulus increases with draw ratio and the absolute values are quite close to those of PE at

the same draw ratio, measured under the same conditions. The modulus of the most highly drawn fibers, 15-20GPa, is high by normal polymer standards and close to commercial high modulus PVA fibers. All indications are that a further increase in draw ratio will produce an increase in Young's modulus.

Acknowledgement The financial support of the Office of Naval Research is gratefully acknowledged. The authors are also indebted to the Kuraray Corporation and Dr. P. Lemstra for the supply of material, and to Dr. Lemstra and Dr. P. Smith for helpful comments.

FIGURE CAPTIONS

Figure 1a Stress - strain curves produced during hot drawing of different concentration D-gels (MW 115,000 powder). Drawing temperature is in the range 111-115°C. Arrows indicated sample fracture. Tests for 3.5% and 15% gels were stopped before fracture.

Figure 1b Stress - strain curves produced during hot drawing of L2, an L-gel of 4.2% concentration, at various temperatures. Arrows indicate sample failure.

Figure 2a Draw ratio as a function of drawing temperature for different concentration D-gels. The draw ratio plotted is the maximum value attained after many trials at each temperature.

Figure 2b Draw ratio as a function of drawing temperature for low concentration gels produced from different starting materials. As in Figure 2a, the draw ratio plotted is the maximum value obtained.

Figure 3a Crystallinity plotted as a function of draw ratio. Points having draw ratio of one represent the isotropic gel before drawing. Crystallinities of the drawn fibers are greater than those of the isotropic gel. When the fibers are melted, the isotropic samples that result have greatly reduced crystallinities. D-series fibers degraded during melting and were not retested.

Figure 3b Crystallinity plotted as a function of drawing temperature for drawn fibers. The dashed lines represent the upper and lower bounds on crystallinity induced by annealing in the same temperature range.

Figure 4a Young's modulus plotted as a function of draw ratio for all gels drawn at 140°C and above.

Figure 4b Young's modulus plotted as a function of draw ratio for gels of concentration less than 5%, drawn at temperatures between 140 and 165°C. This reduced data set produces a better defined relationship. The data for polyethylene fibers, large filled diamonds, are literature values [6] for comparison.

Figure 5 Young's modulus plotted as a function of crystallinity for PVA fibers drawn from gels.

Figure 6a Orientation angle, Φ, of the (110) reflection plotted as a function of draw ratio for fibers of PVA drawn from a number of different gels.

Figure 6b Young's modulus plotted as a function of orientation angle, Φ, for the PVA fibers used in Figure 6a.

Figure 7 Retraction plotted as a function of temperature for fibers having a draw ratio $\lambda = 11.0$. Solid lines connect data points from separate specimens cut from one fiber. Dashed lines connect data points from a single specimen tested by slow heating through the full temperature range.

TABLES

Table 1

concentration %	l_e' nm	d' nm	λ_{th}	λ_{max}	
100.0	14.0	4.65	1.7	6.8	
15.0	93.3	12.0	4.5	11.3	(at 180°C)
9.3	151	15.2	5.7	11.0	
6.2	226	18.7	7.0	12.2	(at 180°C)
4.2	333	22.7	8.5	12.0	
3.8	369	23.9	8.9	12.0	
2.4	584	30.0	11.2	12.2	
2.0	701	32.9	12.3	14.0	

MW 87,000 c^* ≐ 2.8% λ_{th} = 10.4
MW 115,000 c^* = 2.1% λ_{th} = 12.0

Table 2

T_a (°C)	D17, 9.3	D27, 2.0	C17, 3.8	C20, 2.0	L2, 4.2	L5, 2.4	L3, 2.1
			Gel Number, Concentration				
			Crystallinity, %				
No anneal	42	46	46	46	40	41	52
115	43	50	46	49	37	48	52
145	43	50	47	50	44	49	55
160	58	50	56	52	46	50	55
			Melting Point, °C				
No anneal	230	227	229	229	229	228	230
115	229.5	227	229	229	229	229	230
145	230	227	229	229	229	230	230
160	230	227	229.5	230	230	230	230

TABLE 3

Sample	Conc.,%	λ	T_d, °C	T_m, °C	X_c, %	E, GPa
D27	2.0	1.0	-	229	46	-
		8.0	157	236.5	60	9.4
		9.4	132	236	62	6.0
		11.0	152	235	61	10.1
		12.4	145	235	64	15.1
		13.6	155	235	79	19.9
C17	3.8	1.0	-	229	46	-
		6.3	151	236.5	53	4.7
		9.8	116	237	60	8.4
		12.0	140	237	62	10.5
C20	2.1	1.0	-	229	46	-
		11.0	146	235	61	10.9
		11.7	143	234	57	13.1
		13.0	143	237	62	12.6
L2	4.2	1.0	-	230	52	-
		7.2	148	237.5	54	5.2
		8.8	149	237	57	5.3
		10.0	146	237	62	8.6
		10.3	154	239.5	64	7.1
L5	2.4	1.0	-	228	41	-
		9.2	123	237	60	11.3
		9.7	138	237	63	10.1
		11.4	145	236.5	57	8.2
		12.2	148	236	55	11.8
L3	2.1	1.0	-	230	52	-
		12.2	163	237	63	12.4
		14.0	163	237.5	71	17.2

TABLE 4

Sample	Conc.,%	λ	T_d, °C	R	M	M/λ
F1	9.3	11.0	145	0.92	6.1	0.55
D27	2.0	13.6	155	0.92	6.8	0.50
		12.4	145	0.892	5.5	0.44
		11.0	152	0.93	6.5	0.59
D14	2.0	6.0	147	0.91	4.1	0.69
C17	3.8	12.0	140	0.901	5.7	0.48
		6.3	151	0.897	4.1	0.65
C20	2.1	11.0	146	0.936	6.7	0.61
L5	2.4	12.2	148	0.96	8.4	0.69
L3	2.1	14	163	0.999	13.6	0.97
		12.2	163	0.923	6.5	0.54

REFERENCES

1 F.C.Frank, Proc. Roy. Soc. A319 (1970) 127

2 H.Tadokoro, Makromol. Chem. Suppl. 2 (1979) 155

3 T. Ohta, Polym. Engng. Sci. 23 (1983) 697

4 G. Capaccio and I.M. Ward, Polymer 15 (1974) 233

5 P.J. Barham and A. Keller, J. Mater. Sci. 11 (1976) 27

6 G. Capaccio, T.A. Crompton and I.M. Ward, J.Polym. Sci. Polym. Phys. Edn. 14 (1976) 1461

7 A. Zwijnenburg and A.J.Pennings, Colloid Polym. Sci. 254 (1976) 868

8 M.J. Hill, P.J. Barham and A. Keller, Colloid Polym Sci. 258 (1980) 899

9 J.C.M.Torfs and A.J. Pennings, J. Appl. Polym. Sci. 26 (1981) 303

10 P. Smith, P.J. Lemstra, B. Kalb and A.J. Pennings, Polym. Bull. 1 (1979) 733

11 P. Smith and P.J. Lemstra, Colloid Polym. Sci. 258 (1980) 891

12 B. Kalb and A.J. Pennings, J. Mater. Sci. 15 (1980) 2584

13 P. Smith, P.J. Lemstra and H. Booij, J. Polym. Sci., Polym. Phys. Edn. 19 (1981) 877

14 European Patent Application No 82102964.2 (1982)

15 P.J. Barham, Polymer 23 (1982) 1112

16 P.F. van Hutten, C.E. Koning, J. Smook and A.J. Pennings, Polymer Comm. 24 (1983) 237

17 K. Furuhata, T. Yokokawa and K. Miyasaka, J. Polym. Sci. Polym. Phys. Edn. 22 (1984) 133

18 G. Hadziionides, Private communication

19 D.T.Grubb, J. Polym. Sci. Polym. Phys. Edn. 21 (1983) 165

20 A. Peguy and R. StJohn Manley, Polymer Comm. 25 (1984) 39

21 C.G. Cannon, Polymer 23 (1982) 1123

22 I. Sakurada, T. Ito and K. Nakamae, J. Polym. Sci., {C15 (1966) 75

23 L.Z. Rogovina, G.L. Slonimskii, L.S. Gembitskii, Ye.A. Serova, V.A.Grigor'eva and Ye.N. Gubenkova, Vysokomol. Soyed. A15 6 (1973) 1256

24 E. Pines and W. Prins, Macromolecules, 6 (1973) 888

25 V.M. Andreyeva, A.A. Anikeyeva, B.I. Lirova and A.A. Tager, Vysokomol. Soyed. A15 8 (1973) 1770

26 H. Halboth and G. Rehage, Die Angewandte Makromolekulare Chemie 38 (1974) 111

27 S.Matsuzawa, K.Yamaura, and H.Kobayashi, Reports on Progress in Polymer Physics Japan XXIII (1980) 39

28 K. Ogasawara, T. Nakajima, K. Yamaura and S. Matsuzawa, Progr. Colloid and Polym. Sci. 58 (1975). 145

29 K. Ogasawara, T. Nakajima, K. Yamaura and S. Matsuzawa, Colloid and Polym. Sci. 254, (1976). 553

30 K. Yamaura, S. Matsuzawa and Y. Go, Kolloid-Z.u Z.Polymere 240 (1971) 820

31 S.Matsuzawa, K Yamaura and H. Yanagisawa, Kolloid-Z.u Z.Polymere 250 (1972) 20

32 J.G. Pritchard, Poly(vinyl alcohol): Basic Properties and Uses, Gordon and Breach Science Pub., London, 1970.

33 D.T. Grubb, J. Mater. Sci. Letters 3 (1984) 499

34 P. Smith and P.J. Lemstra, Polymer 21 (1980) 1341

35 J. Smook, J.C.M. Torfs and A.J. Pennings, Macromol. Chem. 182 (1981) 3351

36 S.N. Zhurkov, B.Ya. Levin and A.V. Savitskii, Dokl. Akad. Nauk SSSR 186 (1969) 132

37 A.V. Savitskii, B.Ya. Levin and V.P. Demicheva, Vysokomol. Soed. Ser. A 15 (1973) 1286

38 T. Kunugi, A. Suzuki and M. Hashimoto, J. Appl. Polym. Sci. 26 (1981) 1951

39 R.S. Porter, Polym. Prepr. Am. Chem. Soc. Div. Polym. Chem. 12 (1971) 2

40 P.J. Barham and R.G.C. Arridge, J. Polym. Sci. Polym. Phys. Edn. 15 (1977) 1177

41 J.F. Kenney and V.F.Holland, J. Polym. Sci. A1 4 (1966) 699

42 P.J. Flory, J. Amer. Chem. Soc. 78 (1956) 5222

43 A.M.Rijke and L.Mandelkern, J. Polym. Sci. A2 8 (1970) 225

44 K.Yamada, M.Kamezawa and M. Takayanagi, J. Appl. Polym. Sci. 26 (1981) 49

Fig 1a

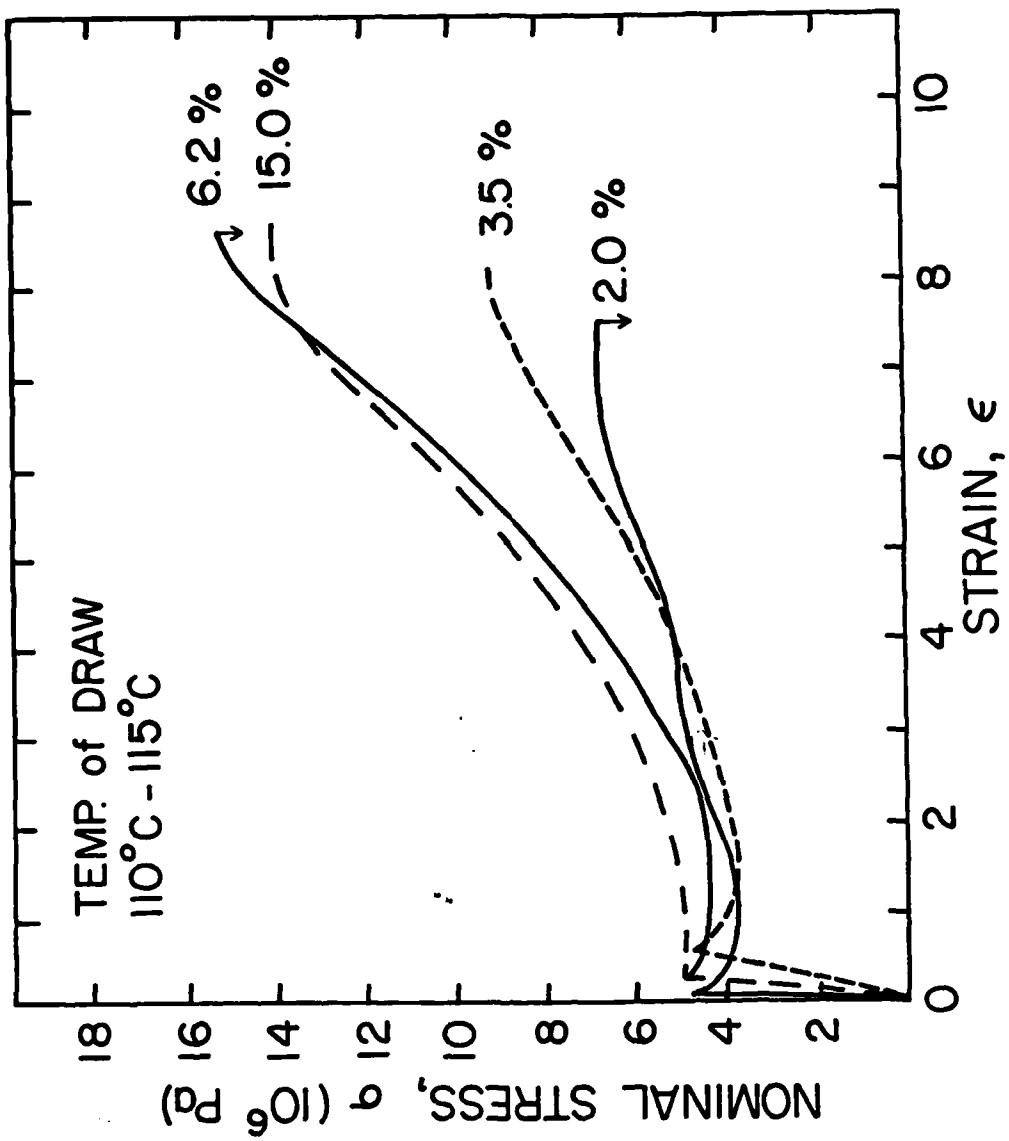
TEMP. of DRAW
110°C - 115°C
6.2 %
15.0 %
3.5 %
2.0 %
NOMINAL STRESS, σ (10⁶ Pa)
STRAIN, ε
0
2
4
6
8
10
2
4
6
8
10
12
14
16
18

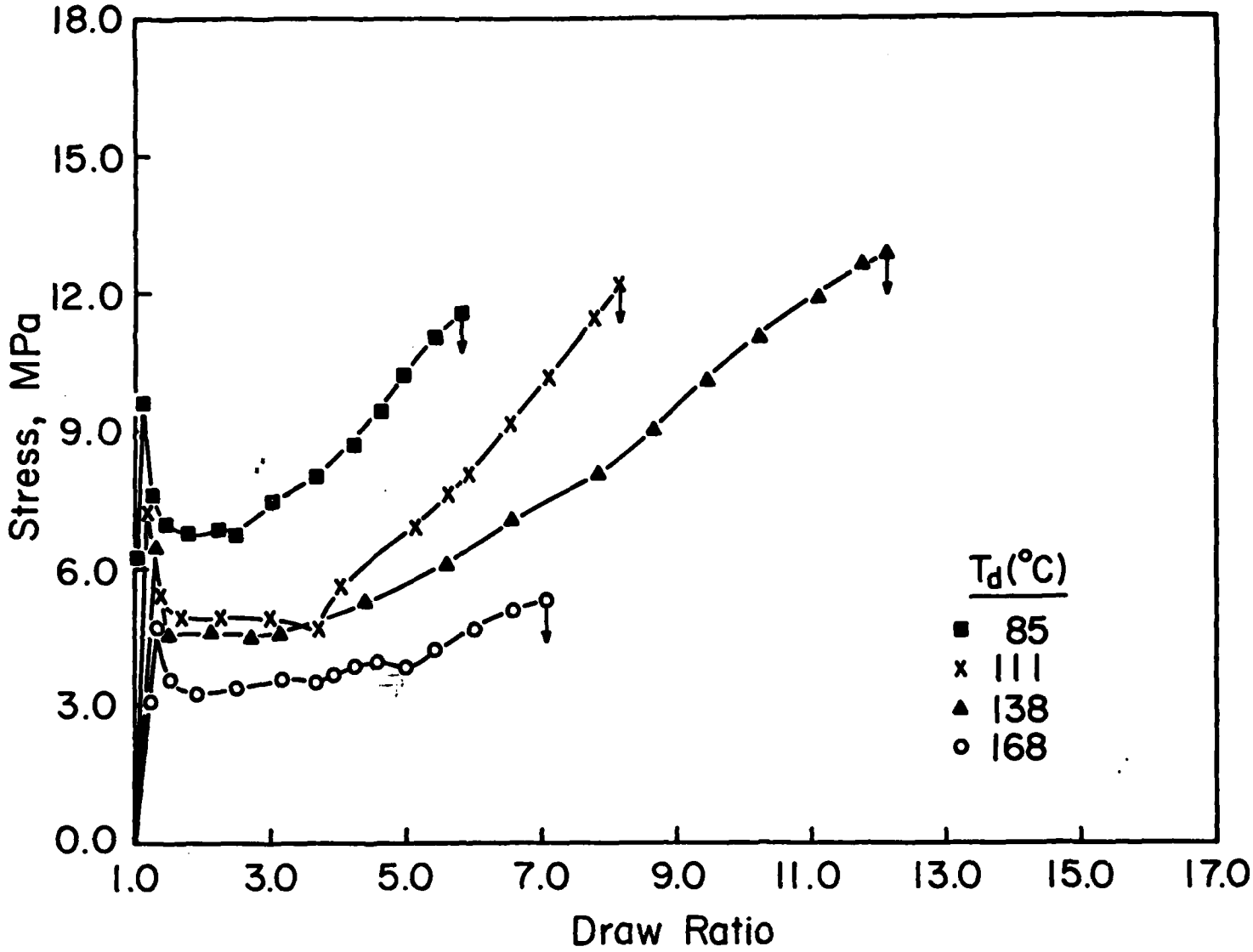
18.0
15.0
12.0
9.0
6.0
3.0
0.0
Stress, MPa
1.0
3.0
5.0
7.0
9.0
11.0
13.0
15.0
17.0
Draw Ratio
T_d(°C)
85
111
138
168

Fig 16

Fig 2a

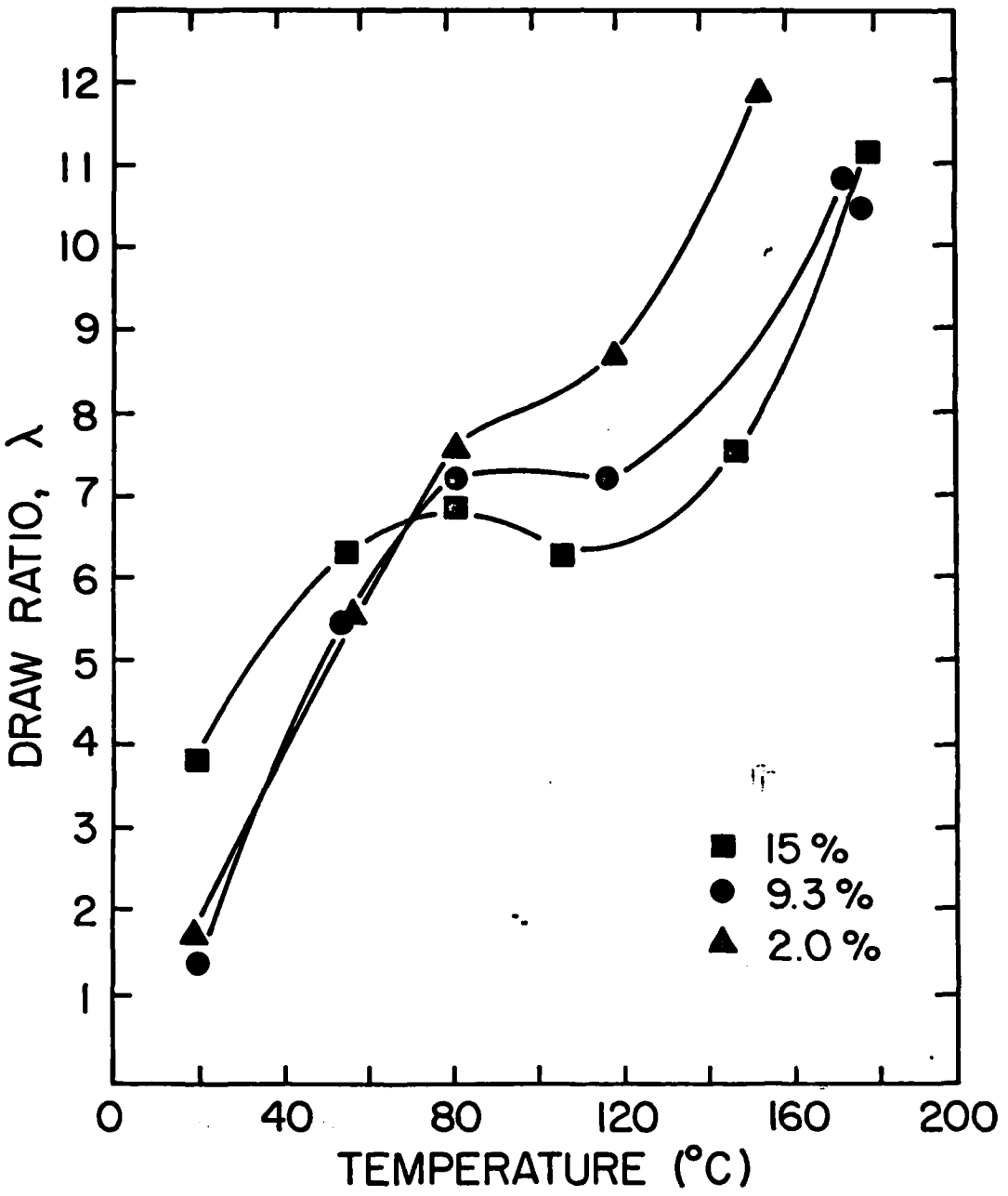
DRAW RATIO, λ
12
11
10
9
8
7
6
5
4
3
2
1
0
40
80
120
160
200
TEMPERATURE (°C)
15 %
9.3 %
2.0 %

Fig 26

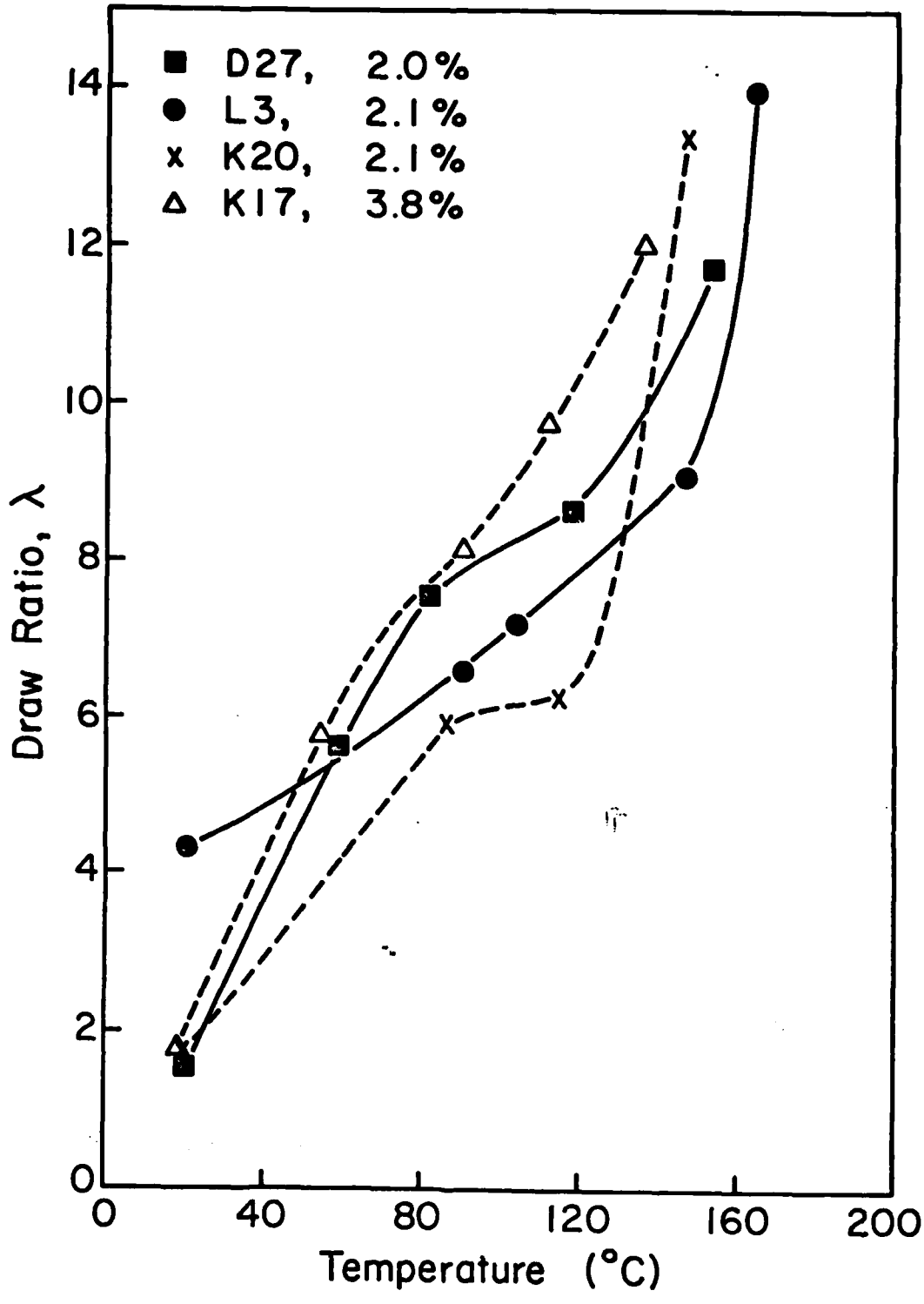
D27, 2.0%
L3, 2.1%
K20, 2.1%
K17, 3.8%
Draw Ratio, λ
0
2
4
6
8
10
12
14
0
40
80
120
160
200
Temperature (°C)

Fig 3c

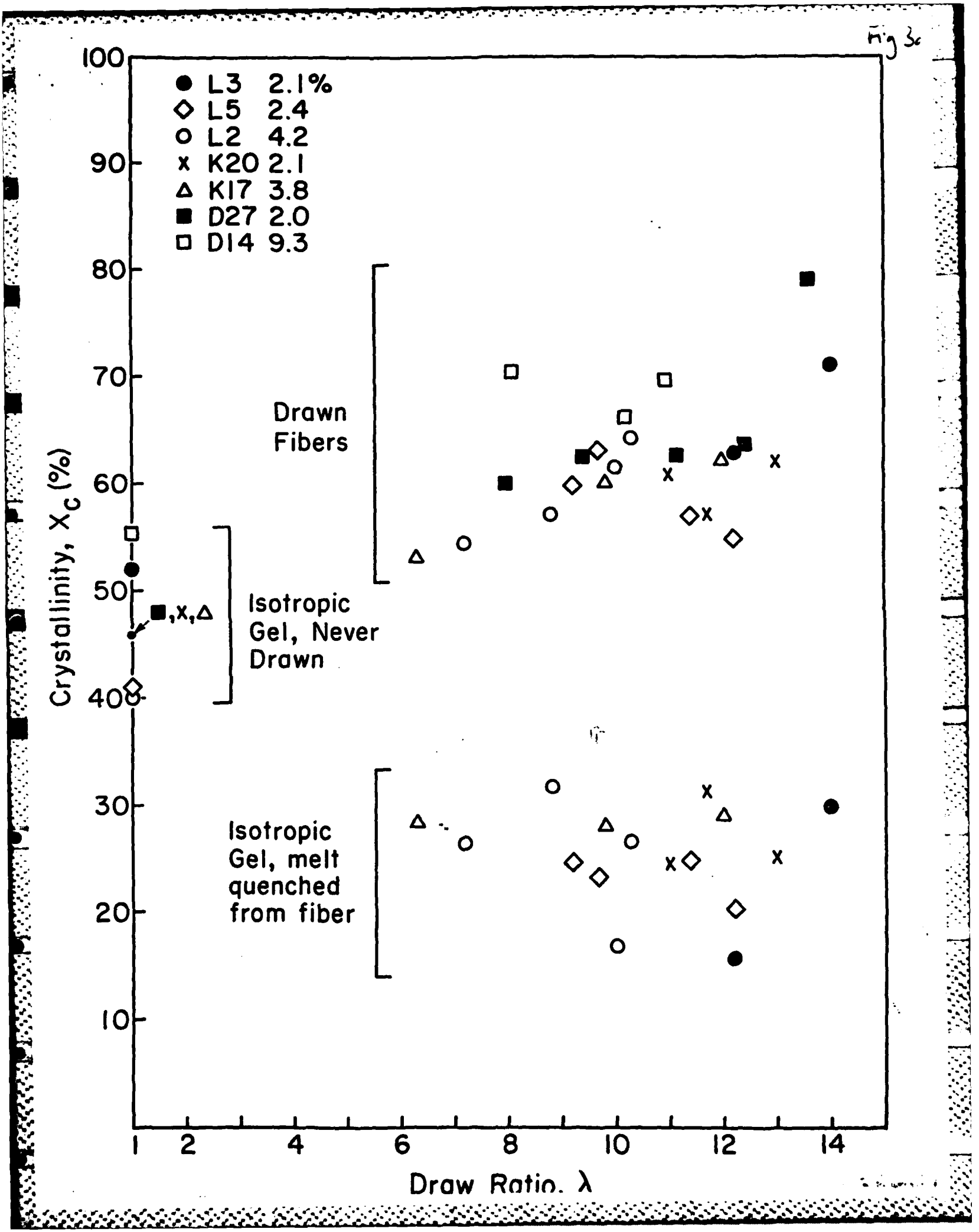
● L3 2.1%
◇ L5 2.4
○ L2 4.2
x K20 2.1
△ K17 3.8
■ D27 2.0
□ D14 9.3
Drawn Fibers
Isotropic Gel, Never Drawn
■,x,△
Isotropic Gel, melt quenched from fiber
Crystallinity, X_c (%)
Draw Ratio, λ
100
90
80
70
60
50
40
30
20
10
1
2
4
6
8
10
12
14

Fig 36

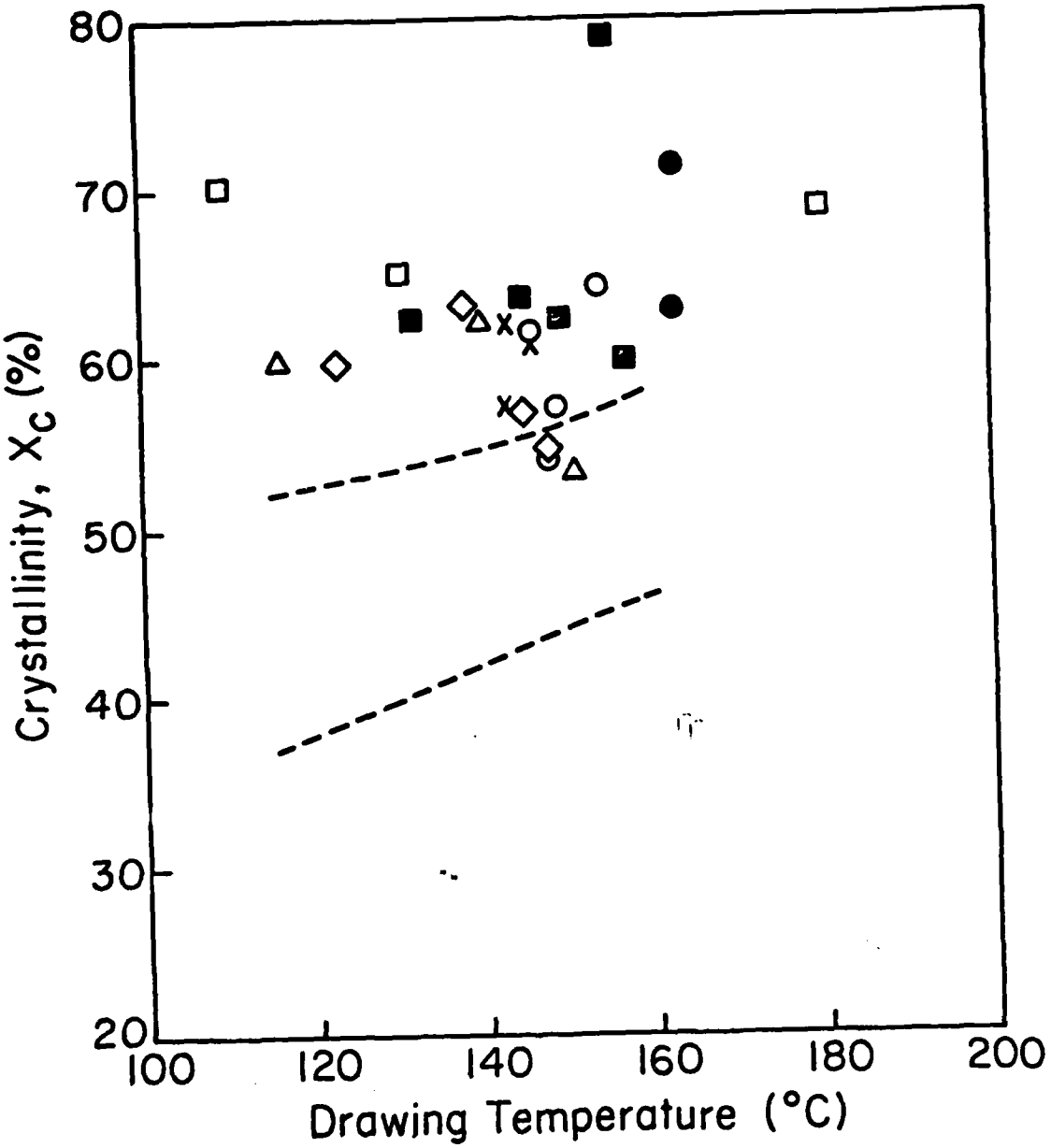
80
70
60
50
40
30
20
100
120
140
160
180
200
Crystallinity, X_c (%)
Drawing Temperature (°C)

Fig 4a

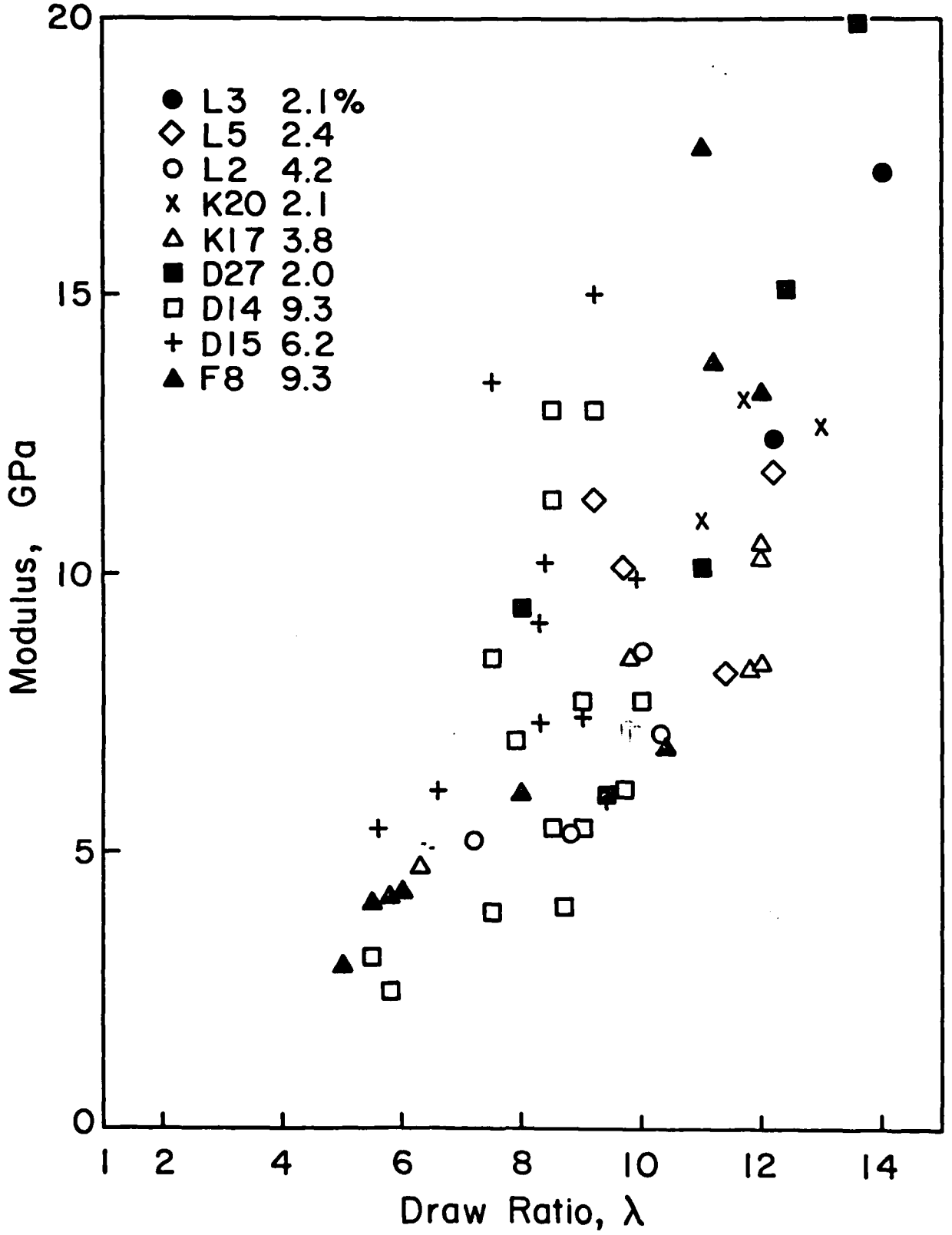
20
15
10
5
0
Modulus, GPa
1
2
4
6
8
10
12
14
Draw Ratio, λ
L3 2.1%
L5 2.4
L2 4.2
K20 2.1
K17 3.8
D27 2.0
D14 9.3
D15 6.2
F8 9.3

Fig 4b

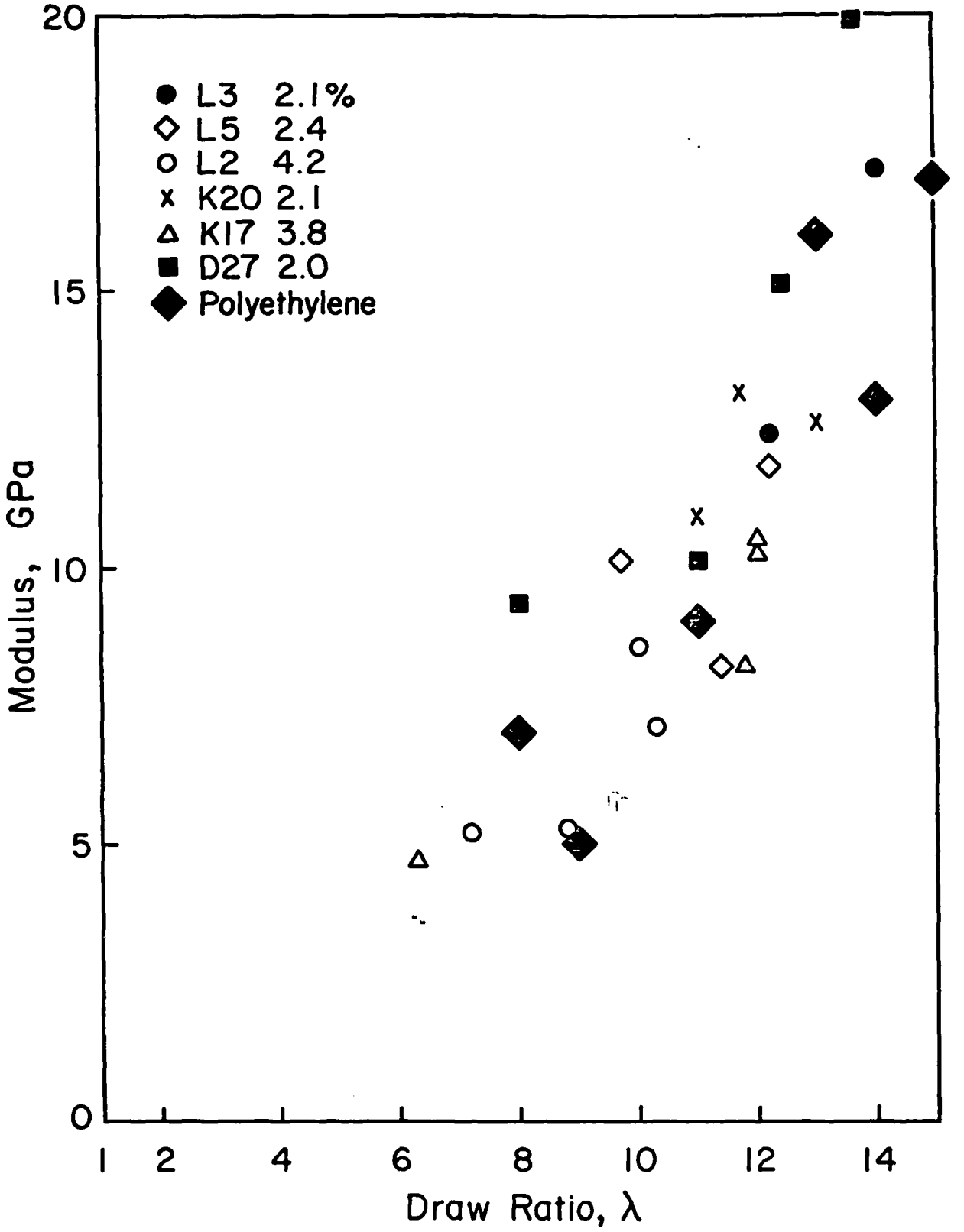
20
15
10
5
0
Modulus, GPa
1
2
4
6
8
10
12
14
Draw Ratio, λ
L3 2.1%
L5 2.4
L2 4.2
K20 2.1
K17 3.8
D27 2.0
Polyethylene

Fig 5

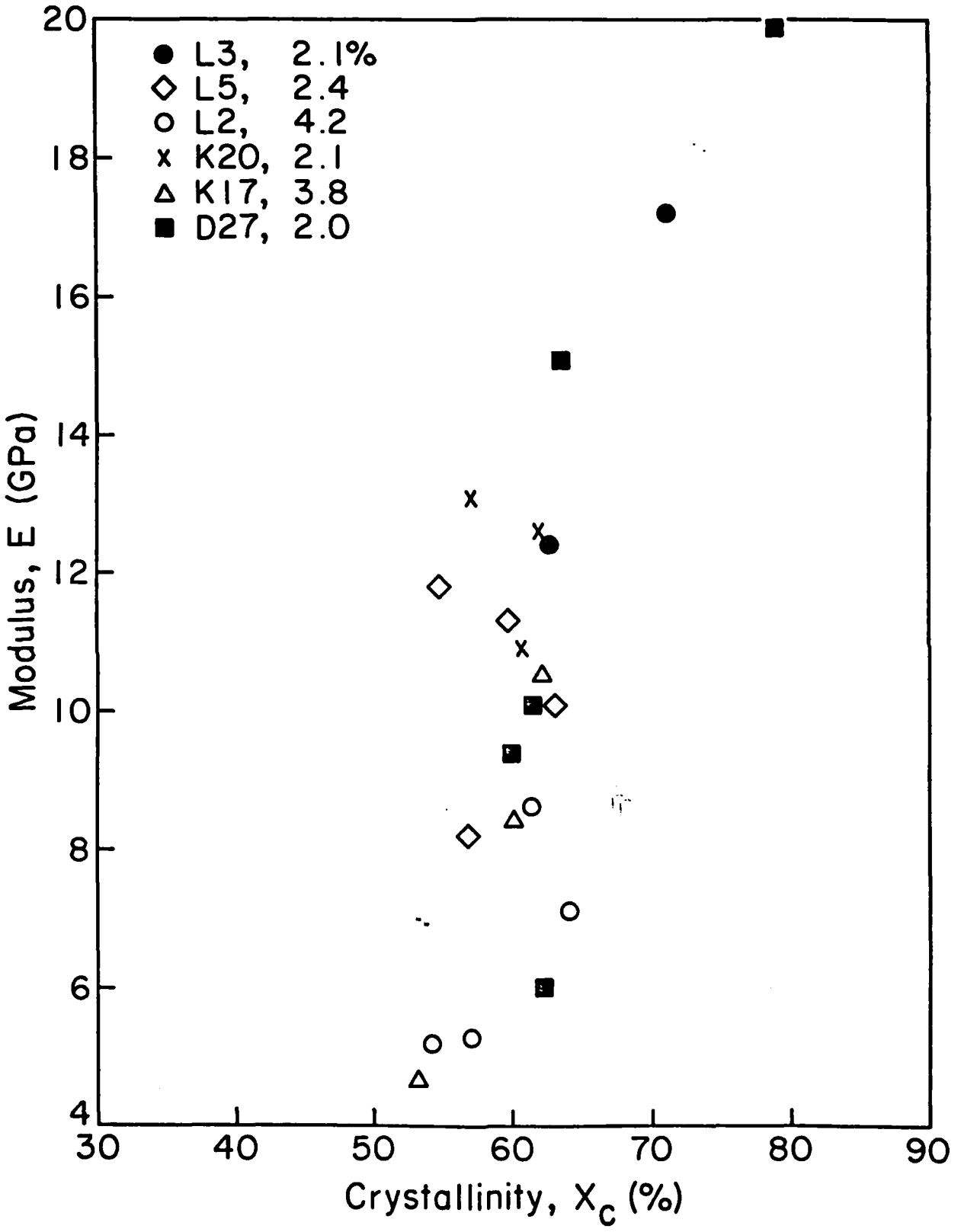
● L3, 2.1%
◇ L5, 2.4
○ L2, 4.2
x K20, 2.1
△ K17, 3.8
■ D27, 2.0
Modulus, E (GPa)
Crystallinity, X_c (%)
20
18
16
14
12
10
8
6
4
30
40
50
60
70
80
90

Fig 6a

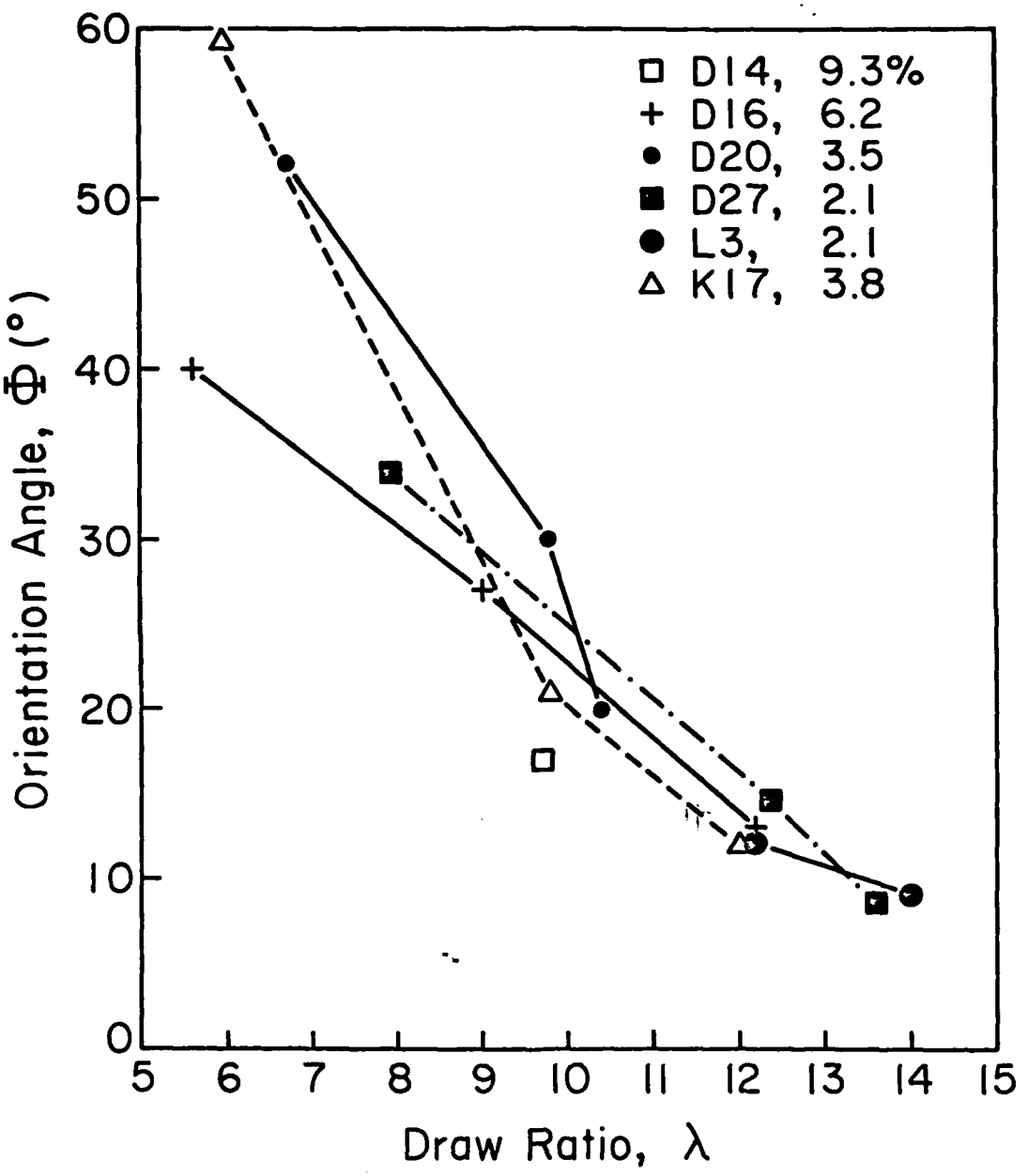
D14, 9.3%
D16, 6.2
D20, 3.5
D27, 2.1
L3, 2.1
K17, 3.8
Orientation Angle, Φ (°)
Draw Ratio, λ
0
10
20
30
40
50
60
5
6
7
8
9
10
11
12
13
14
15

Fig 66

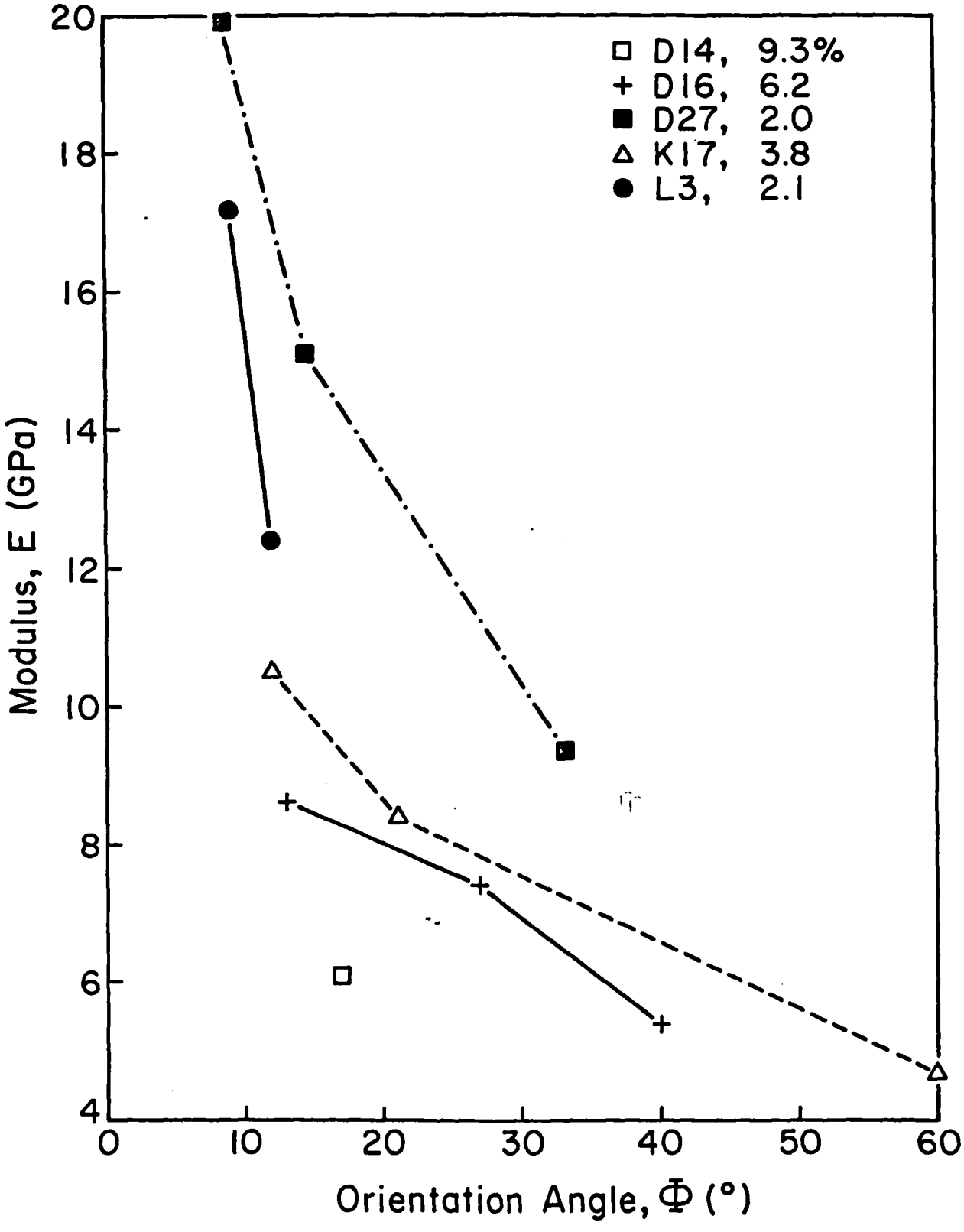
□ D14, 9.3%
+ D16, 6.2
■ D27, 2.0
△ K17, 3.8
● L3, 2.1
Modulus, E (GPa)
20
18
16
14
12
10
8
6
4
0
10
20
30
40
50
60
Orientation Angle, Φ (°)

Fig 7

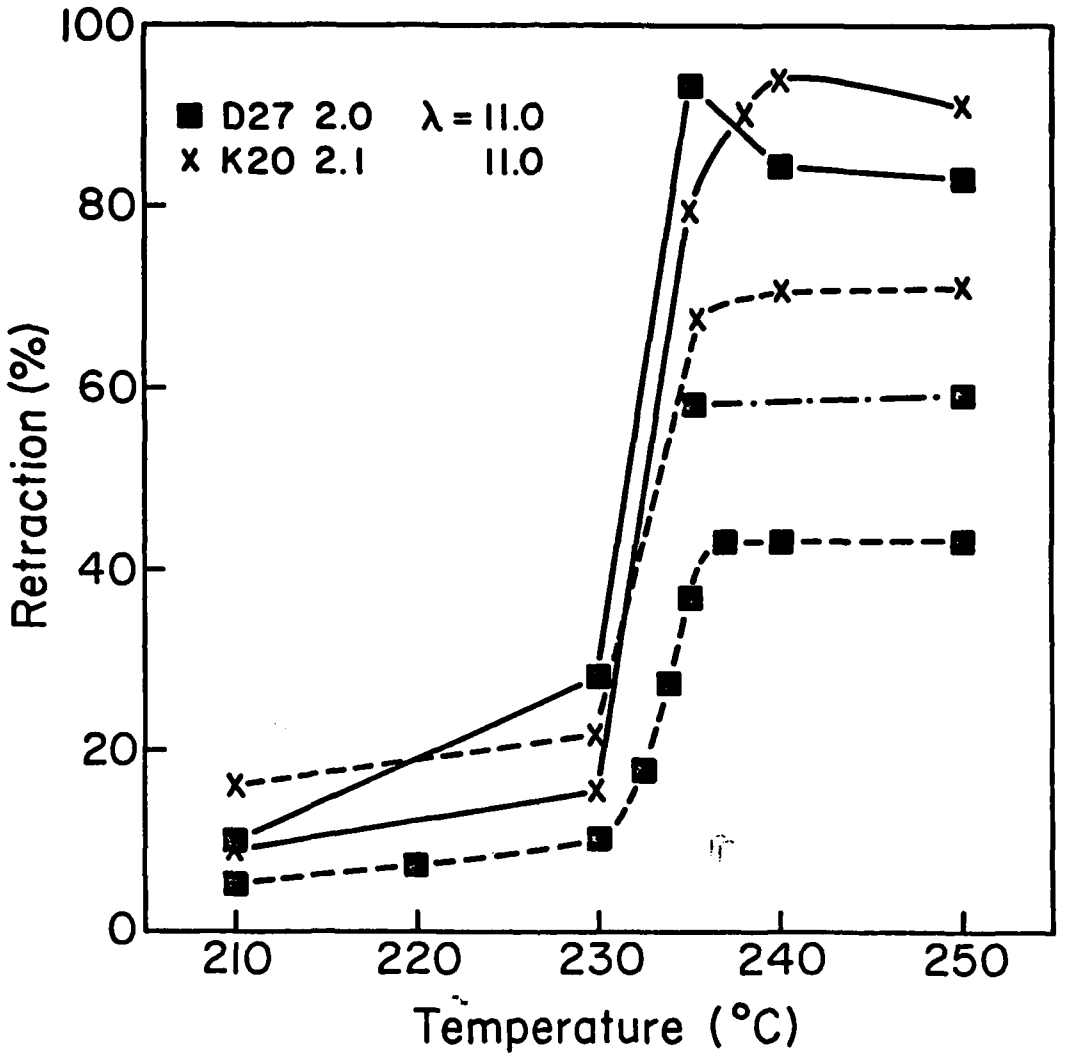
100
80
60
40
20
0
Retraction (%)
■ D27 2.0 λ = 11.0
x K20 2.1 11.0
210
220
230
240
250
Temperature (°C)

DL/413/83/01
GEN/413-2

TECHNICAL REPORT DISTRIBUTION LIST, GEN

	No. Copies
Office of Naval Research Attn: Code 413 800 N. Quincy Street Arlington, Virginia 22217	2
Dr. Bernard Douda Naval Weapons Support Center Code 5042 Crane, Indiana 47522	1
Commander, Naval Air Systems Command Attn: Code 310C (H. Rosenwasser) Washington, D.C. 20360	1
Naval Civil Engineering Laboratory Attn: Dr. R. W. Drisko Port Hueneme, California 93401	1
Defense Technical Information Center Building 5, Cameron Station Alexandria, Virginia 22314	12
DTNSRDC Attn: Dr. G. Bosmajian Applied Chemistry Division Annapolis, Maryland 21401	1
Dr. William Tolles Superintendent Chemistry Division, Code 6100 Naval Research Laboratory Washington, D.C. 20375	1
Dr. David Young Code 334 NORDA NSTL, Mississippi 39529	1
Naval Weapons Center Attn: Dr. A. B. Amster Chemistry Division China Lake, California 93555	1
Scientific Advisor Commandant of the Marine Corps Code RD-1 Washington, D.C. 20380	1
U.S. Army Research Office Attn: CRD-AA-IP P.O. Box 12211 Research Triangle Park, NC 27709	1
Mr. John Boyle Materials Branch Naval Ship Engineering Center Philadelphia, Pennsylvania 19112	1
Naval Ocean Systems Center Attn: Dr. S. Yamamoto Marine Sciences Division San Diego, California 91232	1

DL/413/83/01
356A/413-2

ABSTRACTS DISTRIBUTION LIST, 356A

Naval Surface Weapons Center
Attn: Dr. J. M. Augl, Dr. B. Hartman
White Oak
Silver Spring, Maryland 20910

Professor Hatsuo Ishida
Department of Macromolecular Science
Case Western Reserve University
Cleveland, Ohio 44106

Dr. Robert E. Cohen
Chemical Engineering Department
Massachusetts Institute of Technology
Cambridge, Massachusetts 02139

Dr. R. S. Porter
Department of Polymer Science
and Engineering
University of Massachusetts
Amherst, Massachusetts 01002

Professor A. Heeger
Department of Chemistry
University of California
Santa Barbara, California 93106

Dr. T. J. Reinhart, Jr., Chief
Nonmetallic Materials Division
Department of the Air Force
Air Force Materials Laboratory (AFSC)
Wright-Patterson AFB, Ohio 45433

Professor J. Lando
Department of Macromolecular Science
Case Western Reserve University
Cleveland, Ohio 44106

Professor C. Chung
Department of Materials Engineering
Rensselaer Polytechnic Institute
Troy, New York 12181

Professor J. T. Koberstein
Department of Chemical Engineering
Princeton University
Princeton, New Jersey 08544

Professor J. K. Gillham
Department of Chemistry
Princeton University
Princeton, New Jersey 08540

Professor R. S. Roe
Department of Materials Science
and Metallurgical Engineering
University of Cincinnati
Cincinnati, Ohio 45221

Professor L. H. Sperling
Department of Chemical Engineering
Lehigh University
Bethlehem, Pennsylvania 18015

Professor Brian Newman
Department of Mechanics and
Materials Science
Rutgers University
Piscataway, New Jersey 08854

Dr. Adolf Amster
Chemistry Division
Naval Weapons Center
China Lake, California 93555

Dr. Stuart L. Cooper
Department of Chemical Engineering
University of Wisconsin
Madison, Wisconsin 53706

Professor D. Grubb
Department of Materials Science
and Engineering
Cornell University
Ithaca, New York 14853

Dr. D. B. Cotts
SRI International
333 Ravenswood Avenue
Menlo Park, California 94205

PLASTEC
DRSMC-SCM-O(D), Bldg 351 N
Armament Research & Development
Center
Dover, New Jersey 07801

END

FILMED

2-85

DTIC